Optical nonlinearity studied via anisotropic microstructure: a numerical study on random impedance networks

1998 J. Phys.: Condens. Matter 10 9549

(http://iopscience.iop.org/0953-8984/10/42/020)

J. Phys.: Condens. Matter **10** (1998) 9549–9559. Printed in the UK PII: S0953-8984(98)95129-3

Optical nonlinearity studied via anisotropic microstructure: a numerical study on random impedance networks

M F Law, Y Gu and K W Yu

Department of Physics, The Chinese University of Hong Kong, Shatin, New Territories, Hong Kong, People's Republic of China

Received 15 June 1998

Abstract. Optical nonlinearity is sensitive to the microstructure of materials. When metal clusters are structured on the nanometre scale, they exhibit a strong nonlinear optical response through the local-field and geometric-resonance effects. In this work, we analyse a model of anisotropic microstructure and examine the effect on the optical nonlinearity in the quasi-static limit. To model anisotropic microstructures, a composite medium is conveniently represented by a random impedance network which consists of both metallic and dielectric bonds. For these networks, we performed numerical simulations in which the metallic bonds are assumed to obey the Drude free-electron model. The results show that the absorption peak can be separated from the nonlinearity enhancement peak, and hence that an even larger optical nonlinearity can be achieved than that reported in the literature.

1. Introduction

With the advent of high-power coherent light sources, optical nonlinearity has become a rapidly growing field. A variety of phenomena arise in systems with a nonlinear response. In order to open new possibilities in information processing and transmission, a large optical nonlinearity is desirable [1]. While the search for new materials with a large optical nonlinearity continues, the use of composite materials has been advocated for some time as a means of enhancing the optical nonlinearity. These materials typically consist of small metal particles embedded in a dielectric host. Recently the optical nonlinearity of nanostructured materials has attracted much attention [2]. In particular, metal clusters exhibit a strong nonlinear optical response when they are structured on the nanometre scale, through the local-field and geometric-resonance effects [3]. These composites are also known to give rise to an anomalously large absorption in the infrared spectrum [4–6].

In this work, we analyse a model of anisotropic microstructure, which can be induced by the electrorheological (ER) effect [7]. It was demonstrated that the absorption peak can be separated from the nonlinearity enhancement peak, and hence that the figure of merit can be increased [3]. To examine the effect of microstructure on the optical nonlinearity in the quasi-static limit, we consider the displacement–field response of the form $\boldsymbol{D} = (\epsilon + \chi|\boldsymbol{E}|^2)\boldsymbol{E}$, where ϵ is the (generally complex) dielectric constant and χ is the third-order nonlinear susceptibility. Our aim is to calculate the effective linear and nonlinear optical responses of the composites.

Although the problem of finding the overall response of composites is relatively old, and significant advances have been made, an exact analytic solution is lacking [8]. One of the most fruitful approaches is to invoke the macroscopic concept of local fields, so that the

0953-8984/98/429549+11$19.50

solution of a genuine many-body problem is reduced to the determination of an effective medium. The effective-medium theories have been applied to electrical transport properties of composite materials and the results agree with experimental data [8]. To analyse the optical response, however, it is more convenient to adopt the spectral representation [9, 10].

The spectral representation [9, 10] is a mathematically rigorous formalism of the effective dielectric constant (equation (5) below). It offers the advantage of the separation of material parameters from the geometric information, which is contained in the spectral function $m(s)$. With a given microstructure, $m(s)$ can be evaluated. Moreover, $m(s)$ satisfies a sum rule, which implies that an increase of $m(s)$ in some region must be balanced by a decrease of that in another region. Hence the absorption is directly linked to the behaviour of $m(s)$.

In a recent work [3], the knowledge of $m(s)$ was employed to calculate the effective dielectric constant as well as the optical nonlinearity within the effective-medium approximation. To validate the effective-medium calculations [3], we perform numerical simulations. For numerical simulations, a composite medium is conveniently modelled by a random impedance network. We shall focus only on two-dimensional networks which correspond to thin films. The generalization to three dimensions is straightforward. Note that the problem of solving for the electric field in a dielectric medium in the quasi-static limit is the same problem as solving for that in a conducting medium. The thermodynamic limit corresponds to an infinite network size, which can never be achieved due to the limitation of computer resources. In what follows, ignoring the finite-size effect will be justified.

The organization of the paper is as follows. In the next section (section 2), we define a model of anisotropic microstructure and discuss the dielectric resonance of clusters of a few bonds. Then in section 3 we review the anisotropic effective-medium approximation, which will be used to calculate the effective linear and nonlinear response functions. In section 4, numerical simulations will be performed on random impedance networks; the results will be compared with the effective-medium calculations. In section 5, we present results on the absorption and nonlinearity enhancement for the optical field polarized both parallel and perpendicular to the axis of uniaxial anisotropy. A summary of our results will be given.

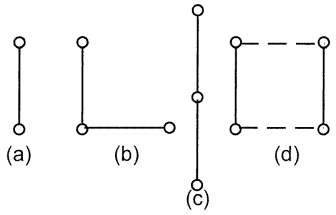

Figure 1. Four types of lattice animals dominant in the dilute limit. (a) A cluster of one bond; (b), (c), (d) clusters of two bonds.

2. The dielectric resonance of lattice animals

To examine the effect of anisotropy on the optical response, we consider uniaxial anisotropic composites, modelled by random-bond-substitution networks [10]. Two independent occupation probabilities $p_{\parallel}$ and $p_{\perp}$ are assigned to the metallic bonds along the parallel and perpendicular directions respectively. In the limit of a small volume fraction p of metallic bonds, the spectral function is dominated by isolated clusters of a few bonds (lattice animals [10, 11]) as shown in figure 1. For example, the probability of occurrence

Table 1. Value(s) of the resonance s of four dominant lattice animals.

Type	Analytic s	Numerical s
(a)	1/2	0.500 000
(b)	$1/\pi$	0.318 310
	$1 - 1/\pi$	0.681 690
(c)	$1 - 2/\pi$	0.363 380
(d)	$2/\pi$	0.636 620

of type (a) clusters depends on the presence of a bond with probability p as well as on the absence of its six nearest-neighbouring bonds with probability $1 - p$. For isotropic networks, the probabilities of occurrence P_i for the four dominant lattice animals are

$$P_a = p(1-p)^6 \qquad P_b = 4p^2(1-p)^8 \qquad P_c = p^2(1-p)^8 \qquad P_d = p^2(1-p)^{10}$$

respectively. In the dilute limit, type (a) clusters give the most pronounced contribution to the spectral density at $s = \frac{1}{2}$ because it is of first order in p. Whereas type (b) clusters contribute a doublet, symmetric about $s = \frac{1}{2}$, type (b), (c) and (d) clusters are of roughly the same strength, proportional to p^2. Analytic expressions for the resonance positions for typical lattice animals and fractal clusters can be found in a recent formalism [10]. The corresponding resonance s values are listed in table 1.

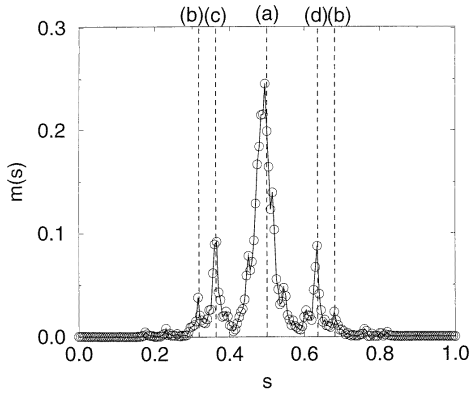

Figure 2. The spectral function for isotropic random impedance networks. Each data point represents an ensemble average for 1000 samples with $L = 15$. The volume fraction $p = 0.02$ and the imaginary part $\eta = 0.002$. The resonance positions are labelled with the respective types of lattice animals.

Figure 2 shows the numerical spectral function (equation (6) below) for isotropic networks with a small volume fraction $p = 0.02$. The resonances for the dominant lattice animals are indicated by dashed lines and labelled with the corresponding types. The numerical spectral function shows a good agreement with a recent calculation using the propagating algorithm [11]. Resonance peaks of small amplitudes other than the dominant ones are due to clusters composed of three or more bonds. Moreover, the contribution of a cluster to the spectral density can be changed substantially by rotating it through 90°. When each of the type (a), (c) or (d) clusters is rotated by 90°, the resulting cluster

becomes decoupled from the applied field and hence there is no contribution to the spectral density [11].

For anisotropic networks, the probabilities of occurrence for the respective lattice animals are modified to

$$P_a = p_\parallel(1-p_\parallel)^2(1-p_\perp)^4 \qquad P_b = 4p_\parallel p_\perp(1-p_\parallel)^4(1-p_\perp)^4$$
$$P_c = p_\parallel^2(1-p_\parallel)^2(1-p_\perp)^6 \qquad P_d = p_\parallel^2(1-p_\parallel)^4(1-p_\perp)^6$$

respectively. Thus by tuning the aspect ratio $p_\perp/p_\parallel$, one can modify the probabilities of occurrence of the different lattice animals and hence the spectral function. For example, increase of the anisotropy would decrease the weight of the type (a) cluster.

3. The anisotropic effective-medium approximation

When an intense dc electric field is applied to a composite medium during the annealing process, the ER effect induces the formation of chainlike anisotropic structures. The degree of anisotropy is characterized by a relation between the occupation probabilities $p_\parallel$ and $p_\perp$ to mimic the structure formation process: $p^2 = p_\parallel p_\perp$. Hence for a given p and $p_\parallel$, $p_\perp$ is calculated from $p_\perp = p^2/p_\parallel$. We calculate the optical response both parallel and perpendicular to the axis of uniaxial anisotropy.

We first solve the problem in the effective-medium approximation (EMA). The coupled EMA self-consistency equations for anisotropic media read [12]

$$p_\parallel\frac{\epsilon_1-\epsilon_\parallel}{\epsilon_1+z_\parallel\epsilon_\parallel}+(1-p_\parallel)\frac{\epsilon_2-\epsilon_\parallel}{\epsilon_2+z_\parallel\epsilon_\parallel}=0 \tag{1}$$

$$p_\perp\frac{\epsilon_1-\epsilon_\perp}{\epsilon_1+z_\perp\epsilon_\perp}+(1-p_\perp)\frac{\epsilon_2-\epsilon_\perp}{\epsilon_2+z_\perp\epsilon_\perp}=0 \tag{2}$$

where $z_\parallel$ and $z_\perp$ are the parameters parallel and perpendicular to the applied dc field; ϵ_1 and ϵ_2 are the constituent dielectric functions; $\epsilon_\parallel$ and $\epsilon_\perp$ are the effective dielectric functions parallel and perpendicular to the applied dc field. In two dimensions (2D), the z-parameters are given by [12]

$$z_\parallel=\frac{\tan^{-1}\sqrt{\epsilon_\perp/\epsilon_\parallel}}{\tan^{-1}\sqrt{\epsilon_\parallel/\epsilon_\perp}} \tag{3}$$

$$z_\perp=\frac{\tan^{-1}\sqrt{\epsilon_\parallel/\epsilon_\perp}}{\tan^{-1}\sqrt{\epsilon_\perp/\epsilon_\parallel}}. \tag{4}$$

In what follows, we simplify our notation using an index $\alpha = \parallel, \perp$. For two-component composites, it has proved convenient to adopt the spectral representation of the effective linear response [9]: let $v = 1-\epsilon_1/\epsilon_2$, $w_\alpha = 1-\epsilon_e/\epsilon_2$ and $s = 1/v$; we find

$$w_\alpha(s)=\int_0^1\frac{m_\alpha(s')\ \mathrm{d}s'}{s-s'} \tag{5}$$

where $m_\alpha(s')$ is the spectral density which is obtained through a limiting process:

$$m_\alpha(s')=\lim_{\eta\to0^+}-\frac{1}{\pi}\operatorname{Im} w_\alpha(s'+\mathrm{i}\eta). \tag{6}$$

Equations (1)–(4) can readily be solved in the spectral representation. In our numerical calculation, we choose the real part at several hundred equally spaced values across the interval $0 \leqslant s' \leqslant 1$, and the imaginary part η to be some small positive value. The actual

value of η is unimportant. We found that $\eta = 0.002$ gives acceptable results by checking the sum rule:

$$\int_0^1 m_\alpha(s')\ \mathrm{d}s' = p_\alpha. \tag{7}$$

We have set $\epsilon_2 = 1$, and ϵ_1 is calculated from $s = s' + \mathrm{i}\eta$.

For isotropic networks, $p_\perp = p_\parallel$, $z_\parallel = z_\perp = 1$ and the EMA self-consistency equations can be solved analytically. The spectral density is given by

$$m(s', p) = \frac{\sqrt{p(1-p) - (s' - \frac{1}{2})^2}}{\pi s'} \tag{8}$$

valid for $0 \leqslant p(1-p) - (s' - \frac{1}{2})^2$. At $p_c = \frac{1}{2}$, we have

$$m(s', p_c) = \frac{1}{\pi}\sqrt{\frac{1-s'}{s'}} \tag{9}$$

which is indeed an exact result by virtue of the duality symmetry in 2D. Other relevant physical quantities can also be calculated from the spectral representation. If a plane-polarized electromagnetic wave of amplitude E_0 with the polarization parallel or perpendicular to the axis of uniaxial anisotropy is incident upon the composite, the local-field averages are given by [3]

$$p\langle E_1^2\rangle_\alpha = \int_0^1 \mathrm{d}s'\ \frac{s^2 m_\alpha(s')}{(s-s')^2} E_0^2 \tag{10}$$

$$p\langle |E_1|^2\rangle_\alpha = \int_0^1 \mathrm{d}s'\ \frac{|s|^2 m_\alpha(s')}{|s-s'|^2} E_0^2. \tag{11}$$

From the average local fields, we calculate the effective nonlinear response through the decoupling approximation [3]:

$$\chi_\alpha |E_0|^2 E_0^2 = p\chi_1 \langle |E_1|^2\rangle_\alpha \langle E_1^2\rangle_\alpha. \tag{12}$$

In this work, only the metallic bond is taken to be nonlinear, i.e., $\chi_2 = 0$. We shall compare the EMA calculations with numerical simulations.

4. Numerical simulation

Consider a random impedance network between two parallel plates at unit potential difference; the effective linear and nonlinear response functions are given by [13]

$$\epsilon_e = \sum_\alpha \epsilon_\alpha\, \delta v_\alpha^2 \tag{13}$$

$$\chi_e = \frac{1}{L^2}\sum_\alpha \chi_\alpha |\delta v_\alpha|^2\, \delta v_\alpha^2 \tag{14}$$

where the summation is over all bonds and δv_α is the (generally complex) potential difference across the bond α, to be solved for when all χ_α are set to zero. We apply Kirchhoff's law to each of the nodes relating the potential of the node (v_ν) to those of its four neighbours (v_μ):

$$\sum_{\mu=1}^{4} \epsilon_\mu (v_\mu - v_\nu) = 0. \tag{15}$$

Applying Kirchhoff's law to all nodes and writing the equations in a matrix form, we obtain a matrix $\mathbf{M}$ of size $L(L-1) \times L(L-1)$; $\mathbf{M}$ consists of nonzero elements along

the five diagonals. This property helps us to optimize the calculation of the inverse $\mathbf{M}^{-1}$. The effective response is obtained by taking an ensemble average over a sufficiently large number of samples.

5. Results and discussion

Both the effective-medium calculations and the numerical simulation are performed on networks in which ϵ_1 is metallic and ϵ_2 is dielectric. The metallic response is assumed to obey the Drude free-electron model:

$$\epsilon_1(\omega) = 1 - \frac{\omega_p^2}{\omega(\omega + \mathrm{i}\gamma)} \tag{16}$$

where ω_p is the plasma frequency and γ is the damping constant. We choose a damping constant $\gamma = 0.1\omega_p$ and $\epsilon_2 = 1.77$ which is the dielectric constant of water for model calculations. The metallic bond is taken to be nonlinear.

We calculate the effective response in four cases of increasing anisotropy: $p_\parallel = 0.1$, $p_\perp = 0.1$ (isotropic case); $p_\parallel = 0.2$, $p_\perp = 0.05$; $p_\parallel = 0.5$, $p_\perp = 0.02$; and $p_\parallel = 0.9$, $p_\perp = 0.011$. We performed numerical simulations on various network sizes. After comparing the results for different network sizes, we conclude that $L = 15$ is sufficient for the present investigation. A further increase in the network size results in no significant difference. This is because the optical response arises from the geometric resonances, rather than from the percolating effects. Each data point represents an ensemble average over 1000 random samples with $L = 15$. The resonance positions of the four types of lattice animals are indicated by vertical dashed lines as a guide to the eye. The probabilities of occurrence for these four lattice animals for various anisotropies are listed in table 2 and table 3.

5.1. The parallel response

For the optical field polarized along the axis of uniaxial anisotropy, we plot the spectral function $m_\parallel(s)$ for four different anisotropies in figure 3. For the isotropic case ($p_\parallel = 0.1$),

Table 2. Probabilities of occurrence of the dominant lattice animals for parallel field.

Type	$p_\parallel = 0.1$, $p_\perp = 0.1$	$p_\parallel = 0.2$, $p_\perp = 0.05$	$p_\parallel = 0.5$, $p_\perp = 0.02$	$p_\parallel = 0.9$, $p_\perp = 0.011$
(a)	0.0531	0.1043	0.1153	0.0086
(b)	0.0172	0.0133	0.0023	0.0000
(c)	0.0043	0.0188	0.0554	0.0076
(d)	0.0035	0.0120	0.0138	0.0000

Table 3. Probabilities of occurrence of the dominant lattice animals for perpendicular field.

Type	$p_\parallel = 0.1$, $p_\perp = 0.1$	$p_\parallel = 0.2$, $p_\perp = 0.05$	$p_\parallel = 0.5$, $p_\perp = 0.02$	$p_\parallel = 0.9$, $p_\perp = 0.011$
(a)	0.0531	0.0185	0.0012	0.0000
(b)	0.0172	0.0133	0.0023	0.0000
(c)	0.0043	0.0006	0.0000	0.0000
(d)	0.0035	0.0005	0.0000	0.0000

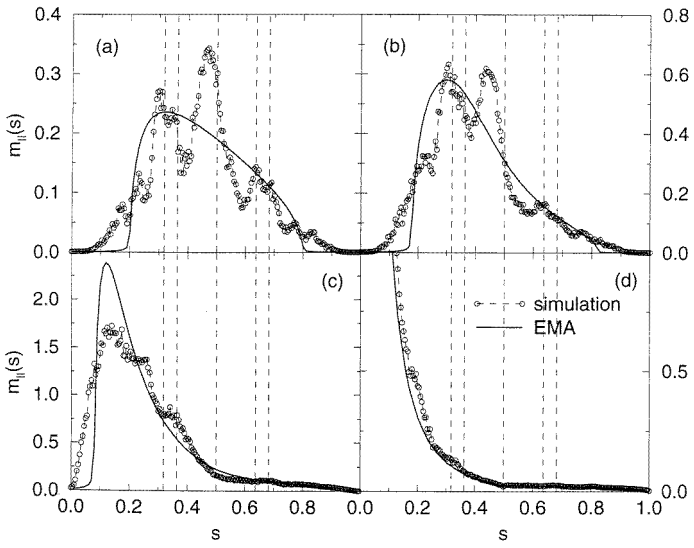

Figure 3. The spectral function for parallel optical field. (a) $p_{\|} = 0.1$, $p_{\perp} = 0.1$, (b) $p_{\|} = 0.2$, $p_{\perp} = 0.05$, (c) $p_{\|} = 0.5$, $p_{\perp} = 0.02$ and (d) $p_{\|} = 0.9$, $p_{\perp} = 0.011$.

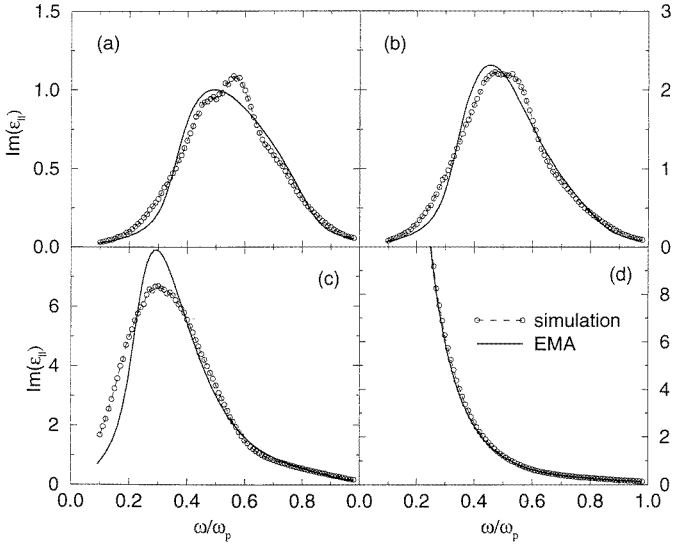

Figure 4. The absorption spectrum for parallel optical field plotted as a function of the frequency ω/ω_p. (a) $p_{\|} = 0.1$, $p_{\perp} = 0.1$, (b) $p_{\|} = 0.2$, $p_{\perp} = 0.05$, (c) $p_{\|} = 0.5$, $p_{\perp} = 0.02$ and (d) $p_{\|} = 0.9$, $p_{\perp} = 0.011$.

the spectral function is well described by the lattice animals limit. However, the resonance peaks are shifted for two reasons. First, the peaks are not symmetric as can be seen from figure 2 and a damping leads to a shift of the peaks. Second, the lattice animals are in fact not isolated; their resonance spectra are affected by clusters in proximity. Hence, even in the lattice animals limit, the EMA cannot reproduce the fine structure of the lattice animals

resonances. It gives instead a broad continuous function. As the anisotropy increases ($p_{\|} = 0.2$), the spectral function is well described by the cluster limit. The peaks are generally larger in height, as expected from table 2 and the sum rule. A further increase in anisotropy ($p_{\|} = 0.5$) results in a red-shift of the spectral density. For the extremely anisotropic case ($p_{\|} = 0.9$), a Drude peak at $s = 0$ indicates that a percolating cluster is formed. The EMA results generally fit the simulation results very well. In the case of large anisotropy, the population of lattice animals becomes negligible, as is evident from table 2. Sharp resonance peaks in the spectral region $0.3 < s < 0.7$ are therefore suppressed.

Next, for the optical absorption spectrum (figure 4), the results are very similar to that for the spectral function. The EMA results generally show a good agreement with the simulation results As the anisotropy increases, the absorption peak shifts to the low-frequency region.

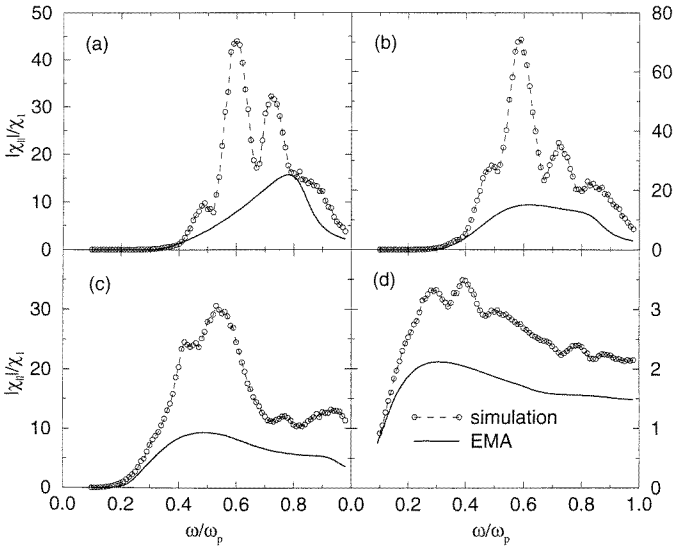

Figure 5. The nonlinearity enhancement spectrum for parallel optical field plotted as a function of the frequency ω/ω_p. (a) $p_{\|} = 0.1$, $p_{\perp} = 0.1$, (b) $p_{\|} = 0.2$, $p_{\perp} = 0.05$, (c) $p_{\|} = 0.5$, $p_{\perp} = 0.02$ and (d) $p_{\|} = 0.9$, $p_{\perp} = 0.011$.

For the parallel effective nonlinear susceptibility as shown in figure 5, the nonlinearity is initially enhanced by the anisotropy ($p_{\|} = 0.2$). A further increase in anisotropy results in a drastic decrease in the nonlinearity ($p_{\|} = 0.5$ and 0.9). The EMA predictions are generally smaller than those of the numerical simulation. The discrepancy is due to the decoupling approximation for analytic calculations of the nonlinear susceptibility. The EMA result may be regarded as a lower bound for the accurate response. Nevertheless, the EMA results agree qualitatively with that of numerical simulation. A red-shift of the nonlinearity enhancement peak is found when the anisotropy increases.

5.2. The perpendicular response

For the optical field polarized perpendicular to the axis of uniaxial anisotropy, we plot the spectral function in figure 6. As expected from equation (7), the spectral function is suppressed progressively as the anisotropy increases. The dominant peak splits into two

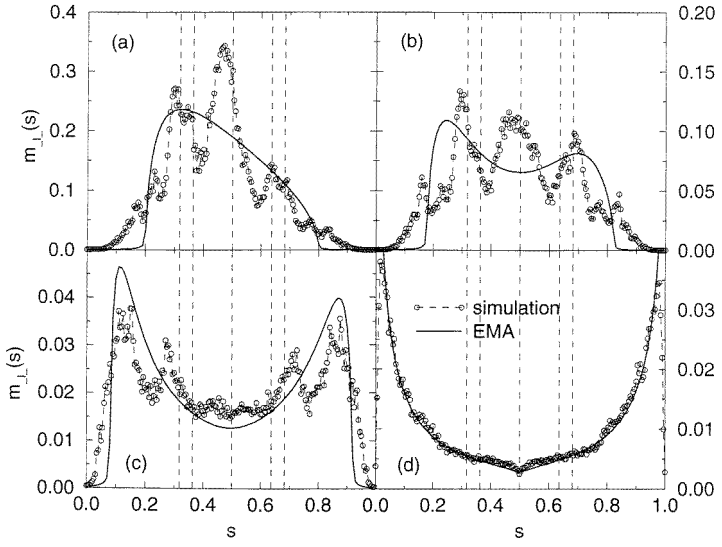

Figure 6. The spectral function for perpendicular optical field. (a) $p_{\|} = 0.1$, $p_{\perp} = 0.1$, (b) $p_{\|} = 0.2$, $p_{\perp} = 0.05$, (c) $p_{\|} = 0.5$, $p_{\perp} = 0.02$ and (d) $p_{\|} = 0.9$, $p_{\perp} = 0.011$.

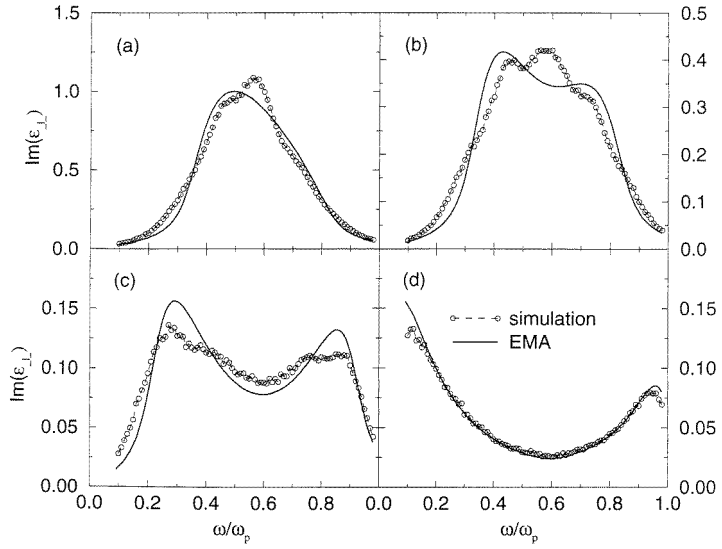

Figure 7. The absorption spectrum for perpendicular optical field plotted as a function of the frequency ω/ω_p. (a) $p_{\|} = 0.1$, $p_{\perp} = 0.1$, (b) $p_{\|} = 0.2$, $p_{\perp} = 0.05$, (c) $p_{\|} = 0.5$, $p_{\perp} = 0.02$ and (d) $p_{\|} = 0.9$, $p_{\perp} = 0.011$.

peaks towards both the high- and low-frequency limits. The decrease of the spectral function in the region $0.3 < s < 0.7$ can be explained using table 3. As the anisotropy increases, the occupation probabilities of the lattice animals decrease monotonically, leading to a trough in the spectral density. There is a peak on the high-frequency side which does not appear in the parallel-field case.

The absorption spectrum (figure 7) is similar to the spectral density. As the anisotropy increases, the absorption is suppressed drastically. A splitting of peaks is also evident. Furthermore, the absorption is larger in the low-frequency region, leading to a red-shift of the overall optical absorption.

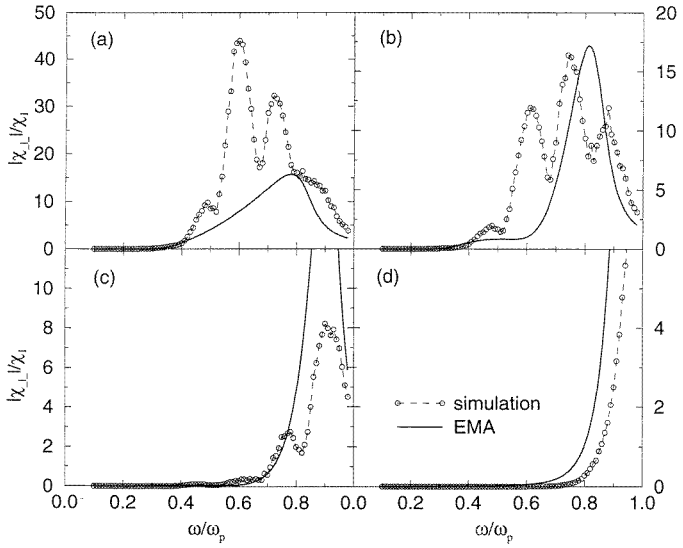

Figure 8. The nonlinearity enhancement spectrum for perpendicular optical field plotted as a function of the frequency ω/ω_p. (a) $p_\parallel = 0.1$, $p_\perp = 0.1$, (b) $p_\parallel = 0.2$, $p_\perp = 0.05$, (c) $p_\parallel = 0.5$, $p_\perp = 0.02$ and (d) $p_\parallel = 0.9$, $p_\perp = 0.011$.

The nonlinear response is plotted as figure 8. As in the parallel-field case, the EMA results agree with the numerical simulation only qualitatively. A blue-shift of the peak is obtained, which is in the opposite direction to that for the absorption.

6. Conclusions

By introducing microstructure into composite materials, the probabilities of occurrence of the lattice animals are modified, resulting in a change of the optical response. In this work, numerical simulations are performed and a comparison with analytic approximation (EMA) is made for the anisotropic microstructure. Previous analytic calculations of the nonlinear response rely on the decoupling approximation, which clearly underestimates the actual nonlinear response. On the other hand, the simulation results are in principle numerically exact. While the analytic EMA linear response agrees reasonably well with the numerical one, it is evident that the decoupling approximation always underestimates the nonlinear response.

For anisotropic microstructures, the optical response is found to be extremely sensitive to the degree of anisotropy. A suppression of the absorption and a concomitant red-shift of the absorption peak are demonstrated. Thus by manipulating the microstructure, the analysis through the spectral representation may give a clear pathway for continuously improving the figure of merit.

In closing, we mention that the predicted enhancement may have relevance to a recent optical-nonlinearity experiment on Au:SiO_2 composites [14], in which a large enhancement

was obtained for annealed samples. Through the separation of the absorption peak from the nonlinearity enhancement peak, it may be possible to achieve even larger optical nonlinearity than that reported in reference [14].

Acknowledgments

This work was supported by the Research Grants Council of the Hong Kong SAR Government under grant number CUHK 4290/98P. KWY acknowledges useful conversation with Professor Ping Sheng.

References

[1] See articles in
Bowden C M and Haus J W (ed) *J. Opt. Soc. Am.* B **6** (a special issue on nonlinear-optical properties of materials)
[2] See articles in
Shalaev V M (ed) 1997 *Nanostructured Materials: Clusters, Composites and Thin Films (ACS Symposium Series 679)* (New York: American Chemical Society)
[3] Yuen K P, Law M F, Yu K W and Sheng P 1997 *Phys. Rev.* E **56** R1322
[4] Tanner D B, Sievers A J and Buhrman R A 1975 *Phys. Rev.* B **11** 1330
[5] Granqvist C G, Buhrman R A, Wyns J and Sievers A J 1976 *Phys. Rev. Lett.* **37** 625
[6] Devaty R P and Sievers A J 1984 *Phys. Rev. Lett.* **52** 1344
[7] See
R Tao and G D Roy (ed) 1994 *Electrorheological Fluids* (Singapore: World Scientific)
[8] Landauer R 1952 *J. Appl. Phys.* **23** 779
[9] Bergman D J and Stroud D 1992 *Solid State Physics* vol 146, ed H Ehrenreich and D Turnbull (New York: Academic) p 147
[10] For discrete network models, see
Clerc J P, Giraud G, Luck J M and Robin Th 1996 *J. Phys. A: Math. Gen.* **29** 4781
See also
Jonckheere Th and Luck J M 1998 *J. Phys. A: Math. Gen.* **31** 3687
[11] Day A R and Thorpe M F 1996 *J. Phys.: Condens. Matter* **8** 4389
[12] Bernasconi J 1974 *Phys. Rev.* B **9** 4575
[13] Stroud D and Hui P M 1988 *Phys. Rev.* B **37** 8719
[14] Liao H B, Xiao R F, Fu J S, Yu P, Wong G K L and Sheng P 1997 *Appl. Phys. Lett.* **70** 1